Available online at www.sciencedirect.com
SCIENCE DIRECT®
Journal of Solid State Chemistry 178 (2005) 41–46
JOURNAL OF SOLID STATE CHEMISTRY
www.elsevier.com/locate/jssc

Syntheses and structures of $CsHo_3Te_5$ and $Cs_3Tm_{11}Te_{18}$ and the electronic structure of $CsHo_3Te_5$

Jiyong Yao[a], Bin Deng[a], Donald E. Ellis[a,b], James A. Ibers[a,*]

[a]Department of Chemistry, Northwestern University, 2145 Sheridan Road, Evanston, IL 60208-3113, USA
[b]Department of Physics and Astronomy, Northwestern University, 2145 Sheridan Road, Evanston, IL 60208-3113, USA

Received 12 July 2004; received in revised form 6 October 2004; accepted 10 October 2004

Abstract

Single crystals of $CsHo_3Te_5$ and $Cs_3Tm_{11}Te_{18}$ have been grown as byproducts in the synthesis of $CsLnZnTe_3$ (Ln = Ho or Tm) through the reaction of Ln, Zn, and Te with a CsCl flux at 850 °C. The crystal structures have been determined from single-crystal X-ray diffraction data. $CsHo_3Te_5$ crystallizes in space group $Pnma$ of the orthorhombic system whereas $Cs_3Tm_{11}Te_{18}$ crystallizes in the space group $C2/m$ of the monoclinic system. Each of the compounds adopts a three-dimensional structure; each possesses tunnels built from $LnTe_6$ octahedra that are filled with Cs atoms. The pseudo-rectangular tunnel in $CsHo_3Te_5$ is large enough in cross-section to accommodate two symmetrically equivalent Cs atoms. In the $Cs_3Tm_{11}Te_{18}$ structure there are two different sized tunnels: the smaller one is only large enough to host one Cs atom per unit cell whereas the larger one can accommodate two Cs atoms. The electronic structure of $CsHo_3Te_5$ was calculated. The band gap is estimated to be about 1.2 eV, consistent with the black color of the crystals.

Keywords: Cesium; Rare-earth; Tellurides; Crystal structure; Synthesis; Electronic structure

1. Introduction

Among ternary alkali-metal rare-earth tellurides there are four different compositions that have been reported: $ALnTe_2$ [1–4], $A_3Ln_7Te_{12}$ [5], $ALnTe_4$ [6–9], and ALn_3Te_8 [9–11]. The $ALnTe_2$ structures have no Te–Te bonds, and hence comprise $A/Ln/Te$ ions in formal oxidation states 1+/3+/2−. Most $ALnTe_2$ compounds crystallize in the trigonal α-$NaFeO_2$ structure type with close-packed Te layers in a pseudocubic arrangement. The octahedral voids are occupied sequentially by A^+ and Ln^{3+} cations. The cubic $LiTiO_2$ structure type is characteristic of some of the $ALnTe_2$ compounds. It consists of cubic closest-packed Te atoms. However, unlike the α-$NaFeO_2$ structure type, the cations in the layers are mixed, alternating between $A^+:Ln^{3+} = 3:1$ and $A^+:Ln^{3+} = 1:3$ in vicinal layers.

The $A_3Ln_7Te_{12}$ compounds adopt a three-dimensional structure; it possesses tunnels built from $LnTe_6$ octahedra that are filled with A atoms. These compounds are also electron precise, with no Te–Te bonds.

The $ALnTe_4$ compounds crystallize in the $KCeSe_4$ structure type [12]. In the structure Ln and Te atoms form two-dimensional anionic layers that are separated by A atoms. The anionic layers themselves are further partitioned into two layers of Te_2^{2-} units sandwiching a layer of Ln^{3+} cations. The closest distances between these Te_2 dumbbells range from 3.7190(2) to 3.781(1) Å, well beyond that of secondary Te–Te interactions. Thus the ionic formulation of the $ALnTe_4$ compounds is $A^+Ln^{3+}(Te_2^{2-})_2$. Some of these compounds display conductivity owing to incomplete carryover of electrons from rare-earth cations to the Te atoms [9].

The ALn_3Te_8 compounds have several polytypes. The simplest crystallizes in the KNd_3Te_8 [11] structure type,

*Corresponding author. Department of Chemistry, Northwestern University, 2145 Sheridan Road, Evanston, IL 60208-3113, USA. Fax: +1 847 491 2976.
E-mail address: ibers@chem.northwestern.edu (J.A. Ibers).

0022-4596/$ - see front matter © 2004 Elsevier Inc. All rights reserved.
doi:10.1016/j.jssc.2004.10.015

which consists of $^{2}_{\infty}[Ln_3Te_8]$ layers separated by A atoms. There are L-shaped triatomic Te_3^{2-} units and infinite $^{1}_{\infty}[Te_4^{4-}]$ zigzag chains in the structure. These ALn_3Te_8 compounds are semiconductors.

Here we report the syntheses and structures of two alkali-metal rare-earth tellurides, $CsHo_3Te_5$ and $Cs_3Tm_{11}Te_{18}$, with stoichiometries different from those above. However, each of these compounds has at least one Se or S analogue, not a common occurrence among ternary tellurides. They both are electron precise and possess discrete Te^{2-} anions. We also report the electronic structure of $CsHo_3Te_5$.

2. Experimental section

2.1. Syntheses

$CsHo_3Te_5$ and $Cs_3Tm_{11}Te_{18}$ were obtained as by-products during the syntheses of the $CsLnZnTe_3$ (Ln = Ho, Tm) tellurides [13]. The starting materials were 0.5 mmol Zn (Johnson Matthey, 99.99%), 1.0 mmol Ho (Alfa Aesar, 99.9%) or Tm (Strem, 99.9%), 2.0 mmol Te (Aldrich, 99.5%), and 1.2 mmol CsCl (Aldrich, 99.99%). The reactants were loaded into fused-silica tubes under an Ar atmosphere in a glove box. These tubes were sealed under a 10^{-4} Torr atmosphere and then placed in a computer-controlled furnace. The samples were heated to 1123 K in 30 h, kept at 1123 K for 96 h, cooled at 4 K/h to 573 K, and then cooled to room temperature. The products consisted of dark-red needles or plates of the $CsLnZnTe_3$ (Ln = Ho or Tm) compounds and black needles of $CsHo_3Te_5$ or $Cs_3Tm_{11}Te_{18}$. The yields were around 5% based on Ln. Analyses of these black needles with an EDX-equipped Hitachi S-3500 SEM showed the presence of Cs, Ln, and Te, but not of Cl or Zn. The compounds are modestly air stable. Efforts to synthesize these compounds in the absence of Zn, using either Cs_2Te_3 or CsCl as flux, were not successful.

2.2. Crystallography

Single-crystal X-ray diffraction data were obtained with the use of graphite-monochromatized Mo$K\alpha$ radiation ($\lambda = 0.71073$ Å) at 153 K on a Bruker Smart-1000 CCD diffractometer [14]. The crystal-to-detector distance was 5.023 cm. Crystal decay was monitored by recollecting 50 initial frames at the end of data collection. For each compound data were collected by a scan of 0.3° in ω to afford 606 frames at each of the ϕ settings 0°, 90°, 180°, and 270°. The exposure times were 10 s/frame for $CsHo_3Te_5$ and 20 s/frame for $Cs_3Tm_{11}Te_{18}$. The collection of intensity data was carried out with the program SMART [14]. Cell refinement and data reduction were carried out with the use of the program SAINT [14] and face-indexed absorption corrections were carried out numerically with the program XPREP [15]. The program SADABS [14] was employed to make incident beam and decay corrections.

The structures were solved with the direct methods program SHELXS and refined with the full-matrix least-squares program SHELXL of the SHELXTL suite of programs [15]. Each final refinement included anisotropic displacement parameters. The program TIDY [16] was then employed to standardize the atomic coordinates in each structure. Additional crystallographic details are given in Table 1 and in Supplementary Material. Tables 2 and 3 present selected bond distances for $CsHo_3Te_5$ and $Cs_3Tm_{11}Te_{18}$, respectively.

2.3. Theoretical calculations

Calculations for $CsHo_3Te_5$ were performed by means of the FP-LAPW method [17,18], as implemented in the WIEN2k code [19]. High-lying semicore states were included as local orbitals. The exchange correlations were treated in the local density approximation (LDA) within density-functional theory by parameterization [20]. The muffin-tin radii were 3.0, 2.8, and 2.85 bohr for Cs, Ho, and Te, respectively. The values of K_{max} and G_{max} were chosen as 7 and 14. These are the plane-wave expansion cutoffs for wave functions and for the densities and potentials, respectively. Open-core treatment was performed on the 4f electrons in order to overcome the shortcomings of the LDA, which always puts the 4f states around the Fermi energy and yields a fractional occupancy. In the open-core treatment the potential was shifted by a constant. The resulting

Table 1
Crystal data and structure refinements for $CsHo_3Te_5$ and $Cs_3Tm_{11}Te_{18}$[a]

	$CsHo_3Te_5$	$Cs_3Tm_{11}Te_{18}$
Formula mass	1265.70	4553.76
a (Å)	23.7076(19)	26.576(2)
b (Å)	4.3604(3)	4.3212(4)
c (Å)	12.8367(10)	20.0864(18)
β (deg)	90	100.453(1)
Space group	*Pnma*	*C*2/*m*
Z	4	2
V (Å^3)	1326.99(17)	2268.5(4)
ρ_c (g/cm^3)	6.335	6.667
μ (cm^{-1})	311.32	349.77
$R(F)$[b]	0.0284	0.0369
$R_w(F_o^2)$[c]	0.0647	0.0905

[a] For both structures, $T = 153(2)$ K and $\lambda = 0.71073$ Å.
[b] $R(F) = \sum ||F_o| - |F_c|| / \sum |F_o|$ for $F_o^2 > 2\sigma(F_o^2)$.
[c] $R_w(F_o^2) = \{\sum[w(F_o^2 - F_c^2)^2] / \sum wF_o^4\}^{1/2}$ for all data. $w^{-1} = \sigma^2(F_o^2) + (z \times P)^2$, where $P = (\mathrm{Max}(F_o^2, 0) + 2 \times F_c^2)/3$; $z = 0.03$ for $CsHo_3Te_5$, and 0.05 for $Cs_3Tm_{11}Te_{18}$.

Table 2
Selected distances (Å) for $CsHo_3Te_5$

Cs–Te2 × 2	3.8276(5)	Ho2–Te1 × 2	3.1269(4)
Cs–Te3 × 2	3.9058(6)	Ho2–Te2	3.0189(5)
Cs–Te4 × 2	4.0052(6)	Ho2–Te3 × 2	2.9925(4)
Cs–Te5	3.8930(8)	Ho2–Te5	3.0424(5)
Ho1–Te1 × 2	3.1314(4)	Ho3–Te1	3.0872(5)
Ho1–Te2 × 2	3.0074(4)	Ho3–Te4 × 2	3.0536(4)
Ho1–Te3	3.0313(5)	Ho3–Te5	3.0097(6)
Ho1–Te4	3.0539(5)	Ho3–Te5 × 2	3.0818(4)

Table 3
Selected distances (Å) for $Cs_3Tm_{11}Te_{18}$

Cs1–Te1 × 2	4.4755(8)	Tm3–Te3 × 2	3.0134(6)
Cs1–Te6 × 4	4.0745(6)	Tm3–Te7	3.0756(9)
Cs1–Te7 × 4	4.0426(7)	Tm3–Te9	3.0715(8)
Cs2–Te3	3.856(1)	Tm4–Te3	3.0678(8)
Cs2–Te4 × 2	3.8326(9)	Tm4–Te5 × 2	2.9673(6)
Cs2–Te5 × 2	3.9223(8)	Tm4–Te6	2.9664(8)
Cs2–Te9 × 2	4.0306(9)	Tm4–Te8 × 2	3.1127(6)
Cs2–Te9	4.159(1)	Tm5–Te3	3.0188(8)
Tm1–Te2 × 2	3.0486(7)	Tm5–Te7 × 2	2.9481(6)
Tm1–Te4 × 4	3.0232(5)	Tm5–Te8	3.0314(8)
Tm2–Te1	2.9907(8)	Tm5–Te8 × 2	3.1643(6)
Tm2–Te2 × 2	3.1183(6)	Tm6–Te1	3.0661(8)
Tm2–Te5	2.9616(8)	Tm6–Te2 × 2	3.1492(6)
Tm2–Te6 × 2	2.9926(6)	Tm6–Te4	2.9634(8)
Tm3–Te1 × 2	2.9835(6)	Tm6–Te9 × 2	3.0135(6)

eigenvalues were also shifted by this same constant. The electron density was not affected at all. The open-core treatment eliminates the problem that 4*f* states show around the Fermi energy level, but the optical transitions related to 4*f* states cannot be studied in this treatment. Brillouin-zone integrations with self-consistency cycles were performed by means of a tetrahedron method [21] with the use of 200*k* points throughout the Brillouin zone. The frequency-dependent optical properties were obtained with the use of the joint density of states (JDOS) weighted by the dipole matrix elements of the optical transitions [22]. In this calculation the allowed and forbidden optical transitions were taken into account.

3. Results and discussion

3.1. Structures

$CsHo_3Te_5$ crystallizes in space group *Pnma* of the orthorhombic system. Each of the atoms has crystallographic symmetry *m*. The shortest Te⋯Te distance is 4.1466(6) Å: thus there are no Te⋯Te interactions. The structure of $CsHo_3Te_5$ (Figs. 1 and 2) is isostructural with that of $CsEr_3Se_5$ [23]. It is a three-dimensional structure possessing Cs-filled tunnels. Each of the three crystallographically unique Ho atoms is coordinated to six Te atoms at the corners of a distorted octahedron. The Ho–Te distances (Table 2) range from 2.9925(4) to 3.1314(4) Å, comparable with those of 3.0230(8)–3.0923(8) Å in $BaHo_2Te_4$ [24]. In the *ac* plane these $HoTe_6$ octahedra stack by edge- and corner-sharing to form a slab with large open cavities. These slabs are connected to each other along the [010] direction by edge sharing to generate a three-dimensional structure that has tunnels in the [010] direction. The pseudo-rectangular tunnel (Fig. 2) is approximately 7.1 × 11.8 Å in rectangular cross-section, large enough to accommodate two Cs atoms. The corresponding tunnel in the isostructural $CsEr_3Se_5$ compound is about 6.7 × 11.8 Å in cross-section. The Cs atoms are surrounded by eight Te atoms at the corners of a bicapped trigonal prism (Fig. 3). Seven Cs–Te bond lengths range from 3.8276(5) to 4.0052(6) Å, comparable with those of

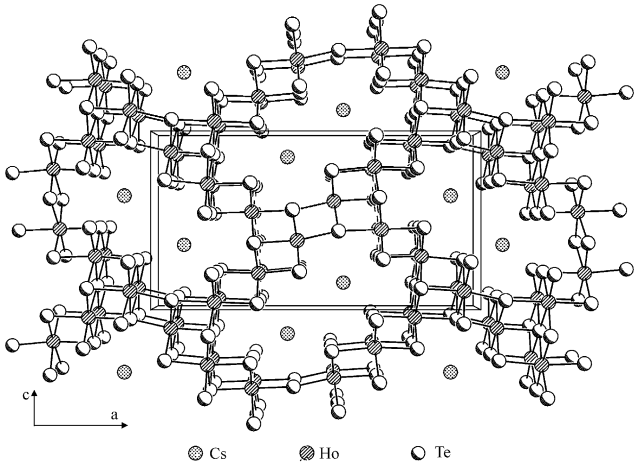

Fig. 1. Structure of $CsHo_3Te_5$.

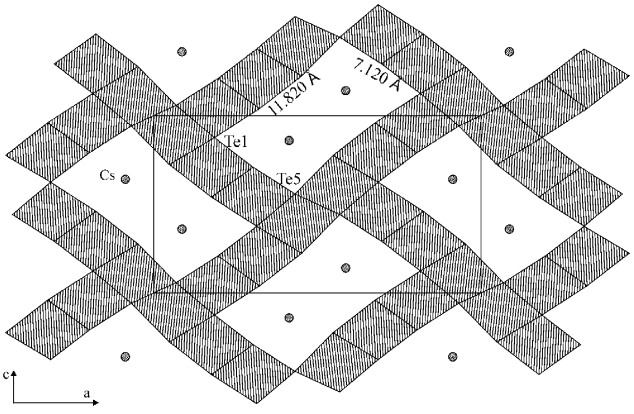

Fig. 2. Polyhedral view of the $CsHo_3Te_5$ structure projected onto the *ac* plane.

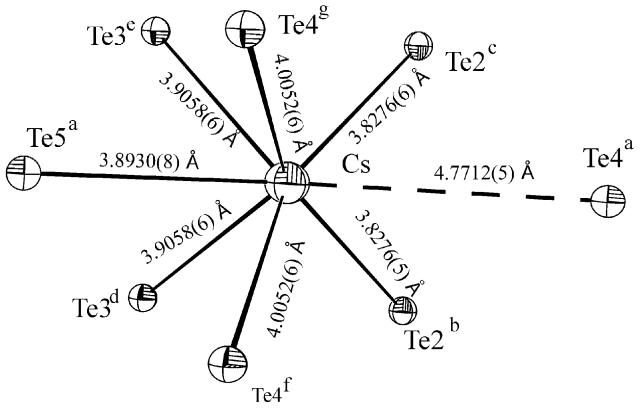

Fig. 3. Coordination geometry of the Cs atom in $CsHo_3Te_5$. (The displacement ellipsoids are shown at the 90% level here and in Figs. 6 and 7.) Symmetry codes: (a) x, y, z; (b) $\frac{1}{2}-x, 1-y, \frac{1}{2}+z$; (c) $\frac{1}{2}-x, -y, \frac{1}{2}+z$; (d) $\frac{1}{2}-x, 1-y, z-\frac{1}{2}$; (e) $\frac{1}{2}-x, -y, z-\frac{1}{2}$; (f) $-x, -y, 1-z$; (g) $-x, 1-y, 1-z$.

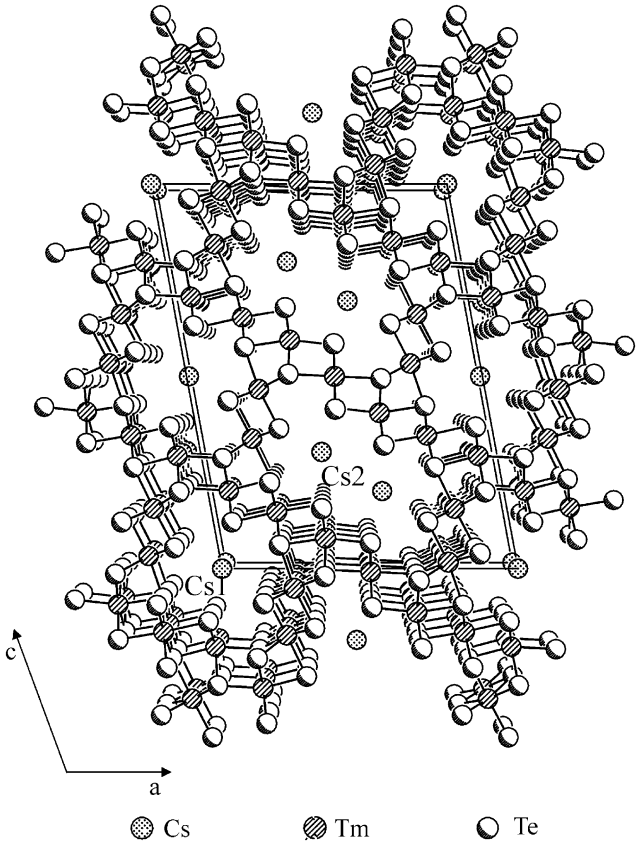

Fig. 4. Structure of $Cs_3Tm_{11}Te_{18}$.

3.693(1)–4.155(2) Å in $Cs_3Tb_7Te_{12}$ [5]. The eighth position is occupied by a Te atom 4.7712(6) Å distant.

The structure of $Cs_3Tm_{11}Te_{18}$ is illustrated in Figs. 4 and 5. It is of the $K_3Cr_{11}S_{18}$ structure type [25], although this is only apparent when the latter structure is transformed to the standard setting through the use of the program TIDY [16]. $Cs_3Tm_{11}Te_{18}$ crystallizes with two formula units in space group $C2/m$ of the monoclinic system. All atoms lie on sites of symmetry m, except for atoms Cs1 and Tm1, which lie on sites of symmetry $2/m$. The structure of $Cs_3Tm_{11}Te_{18}$ is also three-dimensional with Cs-filled tunnels along the [010] direction. The shortest Te···Te distance is 4.001(1) Å. Thus there are no Te–Te bonds in the structure. Each of the crystallographically independent Tm atoms is coordinated to a distorted octahedron of six Te atoms. The Tm–Te distances range from 2.9481(6) to 3.1643(6) Å, similar to those of 2.9987(8)–3.0715(9) Å in $BaTm_2Te_4$ [24]. The $TmTe_6$ octahedra are connected by edge-, face-, and corner-sharing to form a slab with large open cavities in the ac plane. These slabs are further connected to each other along the b direction to complete the three-dimensional structure possessing tunnels in the [010] direction. However, in contrast to the $CsHo_3Te_5$ structure where there is only one kind of tunnel, there are two kinds of tunnels of different sizes in the $Cs_3Tm_{11}Te_{18}$ structure (Fig. 5). The smaller tunnel, about 7.5×7.6 Å in rectangular cross-section, is only large enough to host one unique Cs1 atom, whereas the larger one, which is about $7.2 \text{ Å} \times 11.7$ Å in rectangular cross-section, can accommodate two symmetrically equivalent Cs2 atoms. For comparison, the larger tunnel in $K_3Cr_{11}S_{18}$ is about 5.8×9.4 Å in cross-section, whereas the smaller one is about 5.9×6.0 Å in cross-section. The Cs1 atoms are surrounded by eight close Te atoms at the corners of a square prism with Cs–Te distances of 4.0426(7)–4.0745(6) Å and two capping Te atoms at a further distance of 4.4755(8) Å (Fig. 6). A similar coordination geometry of Cs atom was observed in $CsBi_4Te_6$ [26]. The Cs2 atoms in the larger tunnel are surrounded by eight Te atoms at the corners of a bicapped trigonal prism with Cs–Te distances ranging from 3.8326(9) to 4.1590(10) Å (Fig. 7). The Cs–Te interactions are similar to those of 3.693(1)–4.155(2) Å in $Cs_3Tb_7Te_{12}$ [5]. The Cs1 atoms are more loosely bound to the Te atoms than are the Cs2 atoms, as can be seen both from the Cs–Te distances (Table 3) and the atomic displacement parameters. The equivalent isotropic atomic displacement parameters for atoms Cs1 and Cs2 are 0.0224(2) and 0.0152(2), respectively (Supplementary Material). Thus the Cs1 atoms may "rattle", a process that could lead to low thermal conductivity in this material.

3.2. Electronic structure

In order to understand the distribution of the valence orbitals of each atom near the Fermi level, the total and partial density of states (DOS) of $CsHo_3Te_5$ were calculated, as shown in Fig. 8. The orbitals of Ho (5*d*) and Te (5*p*) dominate the states in the energy range from −5 to 10 eV. Most of the contributions around the

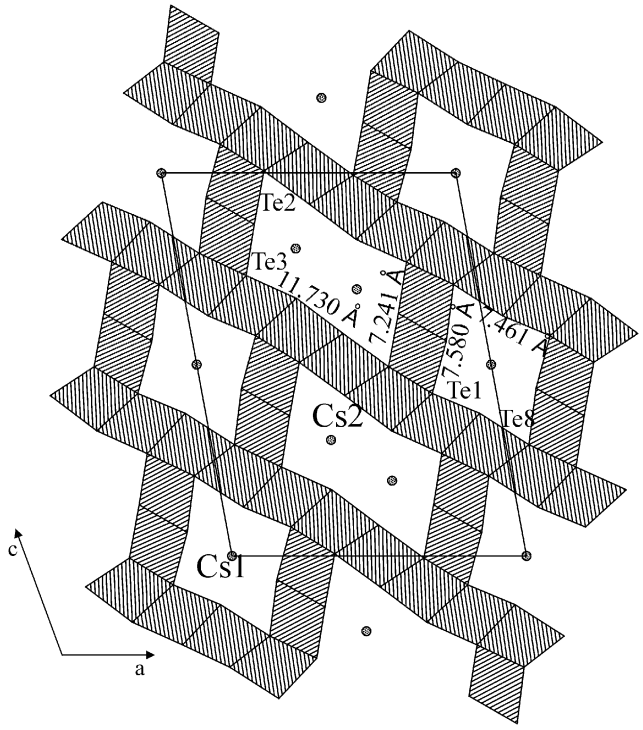

Fig. 5. Polyhedral view of the $Cs_3Tm_{11}Te_{18}$ structure projected onto the *ac* plane.

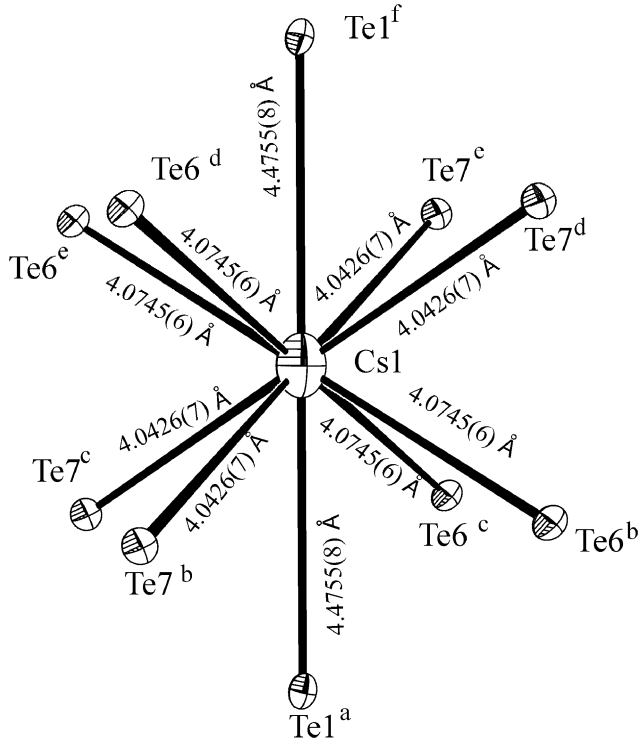

Fig. 6. Coordination geometry of atom Cs1 in $Cs_3Tm_{11}Te_{18}$. Symmetry codes: (a) x, y, z; (b) $\frac{1}{2}-x,-\frac{1}{2}-y,-z$; (c) $x-\frac{1}{2},\frac{1}{2}+y,z$; (d) $\frac{1}{2}-x,\frac{1}{2}-y,-z$; (e) $x-\frac{1}{2},y-\frac{1}{2},z$; (f) $-x,-y,-z$.

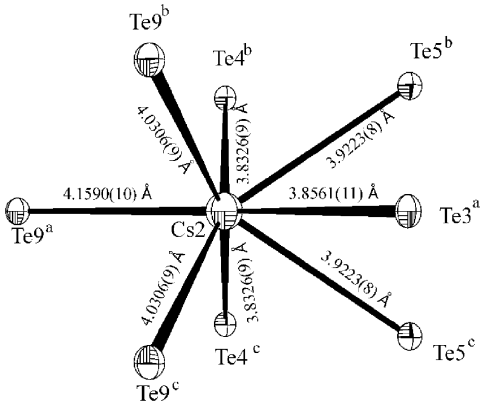

Fig. 7. Coordination geometry of atom Cs2 in $Cs_3Tm_{11}Te_{18}$. Symmetry codes: (a) x, y, z; (b) $\frac{1}{2}-x,\frac{1}{2}-y,1-z$; (c) $\frac{1}{2}-x,-\frac{1}{2}-y,1-z$.

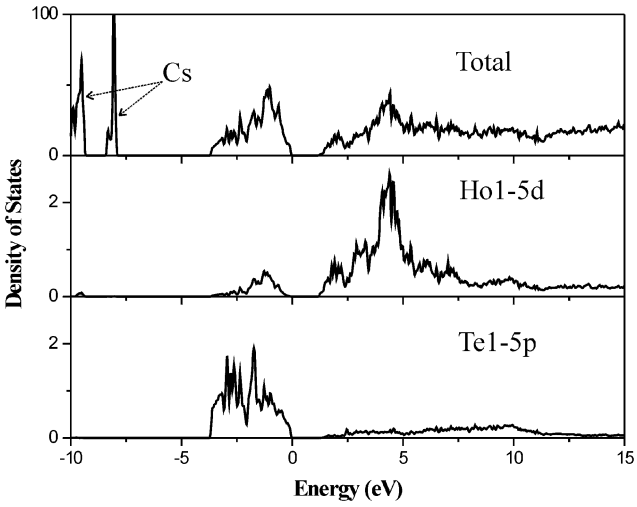

Fig. 8. The total and partial DOS of $CsHo_3Te_5$.

Fermi level are from Te 5*p* electrons and Ho 5*d* electrons. The peaks ranging from −12 to −8 eV originate from Cs(5*s*) states, because these states were treated as local orbitals. Cs(6*s*) orbitals have no significant contributions around the Fermi level. Thus the electronic properties are mainly determined by the three-dimensional $[Ho_3Te_5]$ anionic framework. Analysis of the partial DOS shows that the Ho-5*d* is found mostly in the conduction band, whereas the Te-5*p* lies mainly in the valence band. To estimate the band gap, we calculated the JDOS. The JDOS is related to a convolution over the valence-band and conduction-band DOS functions. It corresponds to the optical transitions between the valence-band and conduction-band states. The JDOS is zero if the transitions are forbidden or if no initial or final states are present at the transition energy. It is large for allowed transitions between bands with a large DOS at the transition energy. From the JDOS (Fig. 9), we estimate this band

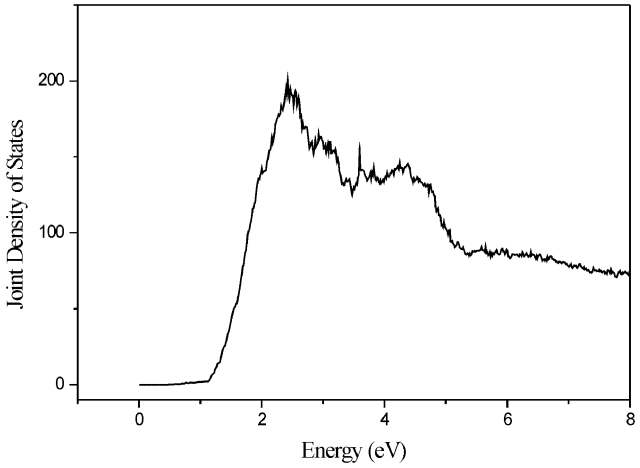

Fig. 9. JDOS of $CsHo_3Te_5$.

gap to be about 1.2 eV, which is consistent with the black color of $CsHo_3Te_5$ crystals.

4. Supplementary material available

Crystallographic data in CIF format have been deposited with FIZ Karlsruhe with the following CSD numbers: $CsHo_3Te_5$, 414225; $Cs_3Tm_{11}Te_{18}$, 414224. These data may be obtained free of charge by contacting FIZ Karlsruhe at +49 7247 808 666 (fax) or crysdata@fiz-karlsruhe.de (email)

Acknowledgment

This research was supported by the MRSEC program of the National Science Foundation (DMR00-76097) at the Materials Research Center of Northwestern University.

References

[1] W. Bronger, W. Brüggemann, M. von der Ahe, D. Schmitz, J. Alloys Compd. 200 (1993) 205–210.
[2] P.M. Keane, J.A. Ibers, Acta Crystallogr. C: Cryst. Struct. Commun. 48 (1992) 1301–1303.
[3] K. Stöwe, C. Napoli, S. Appel, Z. Anorg. Allg. Chem. 629 (2003) 1925–1928.
[4] F. Lissner, T. Schleid, Z. Anorg. Allg. Chem. 629 (2003) 1895–1897.
[5] O. Tougait, H. Noël, J.A. Ibers, Solid State Sci. 3 (2001) 513–518.
[6] W. Bensch, P. Dürichen, Acta Crystallogr. C: Cryst. Struct. Commun. 53 (1997) 267–269.
[7] K. Stöwe, Solid State Sci. 5 (2003) 765–769.
[8] K. Stöwe, C. Napoli, S. Appel, Z. Anorg. Allg. Chem. 629 (2003) 321–326.
[9] K. Stöwe, J. Solid State Chem. 176 (2003) 594–608.
[10] K. Stöwe, Z. Anorg. Allg. Chem. 629 (2003) 403–409.
[11] R. Patschke, J. Heising, J. Schindler, C.R. Kannewurf, M. Kanatzidis, J. Solid State Chem. 135 (1998) 111–115.
[12] A.C. Sutorik, M.G. Kanatzidis, Chem. Mater. 9 (1997) 387–398.
[13] J. Yao, B. Deng, L. J. Sherry, A.D. McFarland, D. E. Ellis, R. P. Van Duyne, J.A. Ibers, Inorg. Chem. (2004), in press.
[14] Bruker, SMART Version 5.054 Data Collection and SAINT-Plus Version 6.45a Data Processing Software for the SMART System, 2003, Bruker Analytical X-ray Instruments, Inc., Madison, WI, USA, 2003.
[15] G.M. Sheldrick, SHELXTL DOS/Windows/NT Version 6.14, Bruker Analytical X-ray Instruments, Inc., Madison, WI, USA, 2003.
[16] L.M. Gelato, E. Parthé, J. Appl. Crystallogr. 20 (1987) 139–143.
[17] E. Wimmer, H. Krakauer, M. Weinert, A.J. Freeman, Phys. Rev. B 24 (1981) 864–875.
[18] M. Weinert, E. Wimmer, A.J. Freeman, Phys. Rev. B 26 (1982) 4571–4578.
[19] P. Blaha, K. Schwarz, G.K. Madsen, D. Kvasnicka, J. Luitz, WIEN2k. An Augmented Plane Wave + Local Orbitals Program for Calculating Crystal Properties, Karlheinz Schwarz, Techn. Universität Wien. Austria, Vienna, 2001.
[20] J.P. Perdew, Y. Wang, Phys. Rev. B: Condens. Matter 45 (1992) 13244–13249.
[21] P.E. Blöchl, O. Jepsen, O.K. Andersen, Phys. Rev. B: Condens. Matter 49 (1994) 16223–16233.
[22] C. Ambrosch-Draxl, J.A. Majewski, P. Vogl, G. Leising, Phys. Rev. B: Condens. Matter 51 (1995) 9668–9676.
[23] S.-J. Kim, S.-J. Park, H. Yun, J. Do, Inorg. Chem. 35 (1996) 5283–5289.
[24] A.A. Narducci, Y. Yang, M.A. Digman, A.B. Sipes, J.A. Ibers, J. Alloys Compd. 303–304 (2000) 432–439.
[25] W. Bronger, C. Herudek, J. Huster, D. Schmitz, Z. Anorg. Allg. Chem. 619 (1993) 243–252.
[26] D.-Y. Chung, T. Hogan, P. Brazis, M. Rocci-Lane, C. Kannewurf, M. Bastea, C. Uher, M.G. Kanatzidis, Science 287 (2000) 1024–1027.